GREEN BANK OBSERVATORY

LASSI: mathematical models and results

Pedro Salas, Paul Marganian, Andrew Seymour, Fred Schwab

June 2, 2020

1 Introduction

The goal of the Laser Antenna Surface Scanning Instrument (LASSI) project is to increase the number of observing hours available at frequencies > 25 GHz for the Green Bank Telescope (GBT). One of the main observing overheads during high frequency observations is that the surface error of the GBT's 100 m primary reflector must be maintained to $\leq \lambda/10$ (300 μm for observations at 100 GHz). The method currently in use to measure and correct the primary's surface during science observations is out-of-focus (OOF) holography (Nikolic et al., 2007). The OOF holography process currently takes 25 minutes (at W-band, 3 mm) to correct the primary's surface to the required accuracy, in a process known as *AutoOOF*. The solutions obtained by *AutoOOF* remain valid for many hours at night. During the day, however, thermal gradients in the antenna backup structure can vary on time scales approaching one hour, requiring calibration measurements at least this often. Using *AutoOOF* would be extremely inefficient, and as a result, observations at high frequency are rarely made during the day.

LASSI's goal is to increase the number of hours available for high-frequency observations through the use of a terrestrial laser scanner (TLS) to measure thermal distortions on the GBT's primary. The TLS is able to map the GBT's primary surface in 3.01 ± 0.04 minutes. Each scan produces a cloud of millions of points, which can be averaged together to produce a map of the primary's surface with an accuracy that is better than the surface rms (≈ 230 μm; Frayer et al., 2018). Frayer et al. (2018) measure an aperture efficiency of 39% at 80 GHz for a surface error of 230 μm.

As described in the concept of operations document for this project (ConOps), the corrections derived from the TLS maps will be relative to a reference scan. The reference scan is obtained with the TLS after the primary's surface has been corrected to its optimal shape by the use of *AutoOOF*. When additional corrections to the surface are required, a new TLS scan (signal scan) will be compared to the reference scan and corrections will be derived from the difference between them (deformation map).

The corrections derived from the difference between the signal and reference scans will be expressed in terms of Zernike polynomials. Zernike polynomials describe common aberrations in optical systems, and are orthogonal over the unit circle (e.g., Born et al., 1999). The active surface of the GBT can handle corrections in terms of Zernike polynomials. Throughout this document we will use the Noll convention to index Zernike polynomials. The active surface of the GBT uses a convention in which the the sign of the azimuthal degree is reversed with respect to Noll, and the first index is 1.

This document presents some preliminary experiments performed with the TLS installed on the GBT. These experiments address; How long does the surface error of the telescope remain below 230 μm? How long does a reference scan remain valid? What factors influence the measurements performed with the TLS? How accurate are the TLS measurements?

When we measure the primary's surface using the TLS we also include the uncertainty associated with the TLS. We will refer to this combined uncertainty as the LASSI noise, i.e. the surface error plus the TLS noise. Given the concept of operations, the corrections to the active surface derived with the TLS will be obtained from the difference between a signal and reference scans. For this reason, we will not directly measure the LASSI noise, but the root mean square (rms) of the difference between scans (scan-to-scan rms). The scan-to-scan rms is a factor of $\sqrt{2}$ larger than the LASSI noise when there are no thermal deformations of the primary. Here we will use the scan-to-scan rms as a proxy for the LASSI noise when indicated.

2 Observations

For the observations presented here the TLS was mounted on top of the receiver cabin of the GBT, facing the main reflector. This position is approximately where the TLS will be mounted during science operations.

2.1 24 hour scan

These scans were performed during June 11 and 12, 2019. The telescope was at its access position (73°) and the TLS continuously scanned the primary's surface for 24 hours. During the scan the active surface of the GBT was commanded to compensate for the zero level of the actuators (determined using radio holography; Hunter et al. 2011), but no corrections were applied to compensate for gravity or thermal deformations. During the day time portions of the 24 hour scan the Sun directly illuminated the GBT's primary surface.

2.2 Injection of known deformations

This experiment was performed during March 27, 2019. The experiment consisted of two scans. The first scan was used as a reference, with the primary's surface unmodified from its nominal shape at the access position. After the reference scan a deformation was introduced into the active surface of the primary. The active surface of the telescope was commanded to reproduce a Zernike polynomial of index 6 (vertical astigmatism) with an amplitude of 1.7 mm. After injecting this deformation to the primary's surface we performed another scan using the TLS, a signal scan.

2.3 OOF holography data from science projects

We searched the last two years of GBT observations for projects that had used the *AutoOOF* procedure. This procedure automatically takes the necessary observations to perform OOF holography and correct the surface of the GBT for gravitational and thermal distortions not included in the gravity model. A total of 3728 projects had been observed at the time we searched the archive (including commissioning projects), 265 of these projects used *AutoOOF* to determine Zernike polynomials up to index 21 (radial order 5). From the results of *AutoOOF* we extracted the mean coefficients of the corrections applied to the active surface of the GBT.

3 Data preprocessing

Preprocessing of the point cloud generated by the TLS is necessary to obtain meaningful results. During our preprocessing we closely follow Holst et al. (2012).

3.1 Object segmentation

The TLS scans a solid angle close to 3.5π and has a range of ≈ 200 m. For these reasons the point cloud includes objects other than the 100m primary surface, e.g., the feed arm and the ground. To remove these unwanted objects we apply cuts in the radial direction and in altitude. These cuts effectively isolate the 100m primary in the point cloud.

3.2 Data reduction

The 100m primary's point cloud consists of roughly eight million points unevenly sampled. If we use an unevenly sampled surface to estimate surface parameters this can bias the results, as shown theoretically by Holst et al. (2014) and empirically by Holst et al. (2015). This is because areas with higher sampling densities have a higher weight on the derived parameters. Thus, when estimating parameters of a surface with unknown deformations it is desirable to reduce the number of data points and produce an evenly sampled cloud of data points.

Here we grid the point cloud to an evenly sampled grid of 512×512 (with an ≈ 20 cm spacing between points). To determine the value at each point in the evenly sampled grid we use a Gaussian kernel and work in spherical coordinates. The spherical smoothing is performed using a GPU. Data gridding and smoothing has the added benefit of reducing the uncertainty of each data point, as well as reducing the number of elements in the point cloud.

3.3 Surface masking

The primary surface of the GBT consists of 2004 panels. Due to faulty actuators, some of the panels can show displacements as large as 50 mm. Also, between some of the panels there are holes which give the reference retroreflectors a clear view of the receiver cabin. The retroreflectors are located 5 mm below the primary's surface. Retroreflectors and panels with large displacements decrease the accuracy to which we can recover surface deformations. To mitigate their effect during the measurement of surface distortions, these are masked using a distance based threshold.

3.4 Rotation and translation of the data

A rotational paraboloid is described by a single parameter, its focal length, when its rotation axis coincides with the z-axis of the coordinate system. This is not the case in the reduced point cloud, so we incorporate two rotations around the x and y axes as well as three translations into the model that describes the primary's parabolic surface. The parameters of the parabolic surface are determined from a least-squares fit of the point cloud to a rotated translated paraboloid. Using the derived rotation angles and translations we align the reduced point cloud with the reference system that corresponds to the primary surface of the telescope. The surface deformation analysis is performed in this reduced and aligned point cloud.

4 Results

4.1 AutoOOF Zernike polynomials

AutoOOF can generate corrections for the first 36 Zernike polynomials. Of these, the first three correspond to corrections that are applied to the secondary surface of the GBT (focus, vertical and horizontal tilts). The remaining terms are corrected for using the active surface on the GBT's primary.

From the last two years of science observations we determined the mean of the corrections applied to the primary surface. We only collected corrections that determined Zernike polynomials up to index 21. We did not collect solutions for higher index polynomials as these are insignificant compared to the first 10 polynomials.

The mean coefficients of the *AutoOOF* generated corrections are presented in Figure 1. The dominant terms are the Zernike polynomials of index 4, 5 and 10 with coefficients of 101 μm, -94 μm and 89 μm.

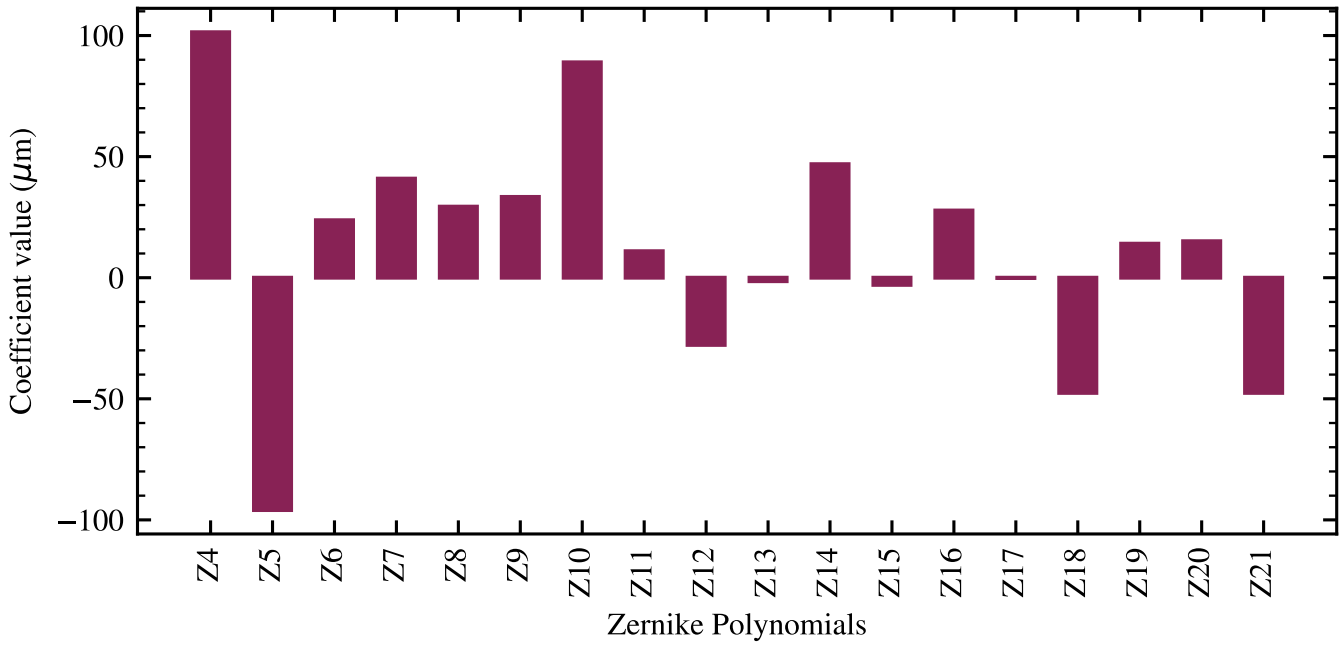

Figure 1: Average of the coefficients of the corrections applied to the primary surface of the GBT during the last two years. These corrections are derived using *AutoOOF*. The corrections are characterized as a linear combination of Zernike polynomials.

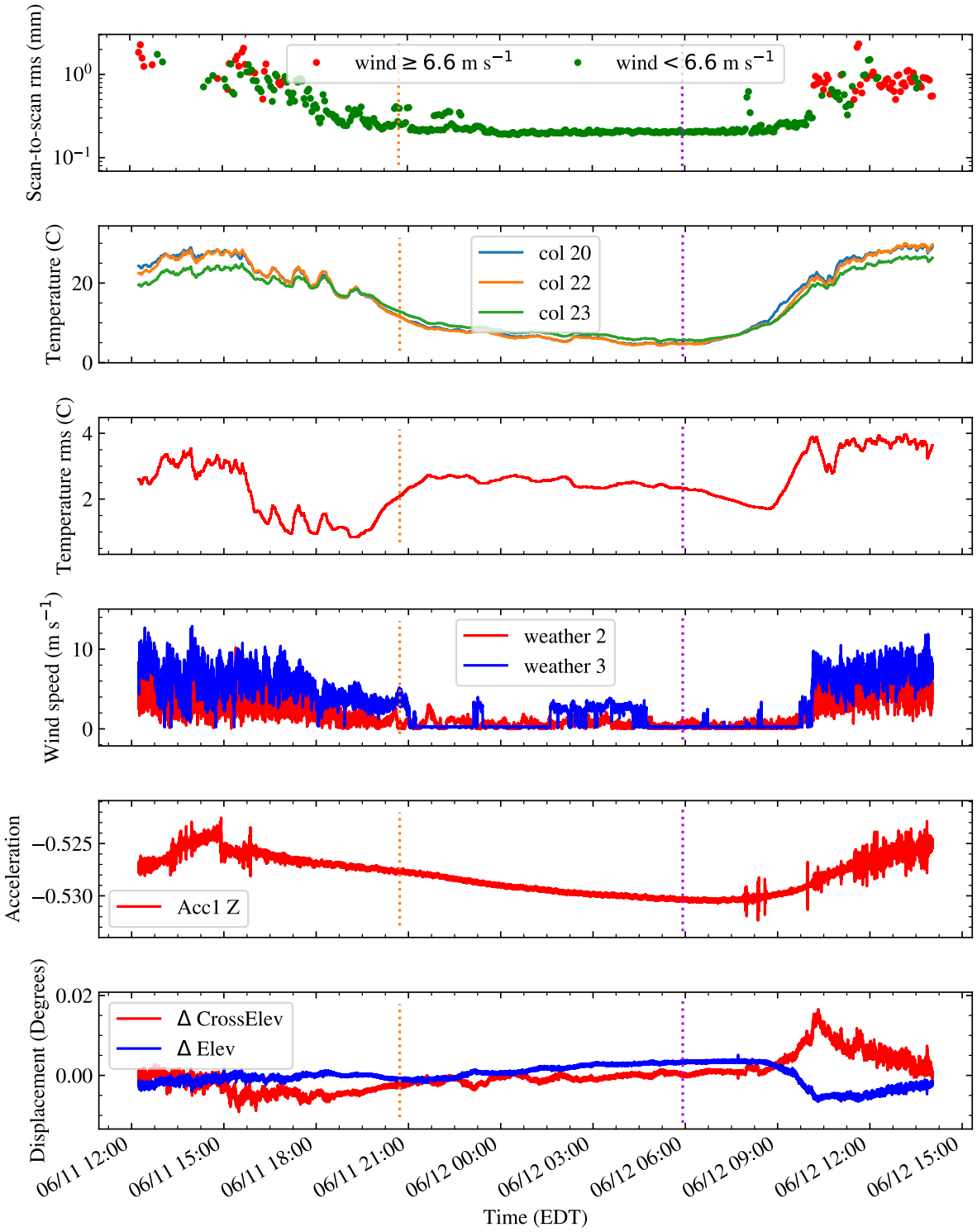

Figure 2: Results from the 24 hour scan performed during June 11 and 12, 2019. From top to bottom; primary reflector scan-to-scan rms; temperature of the primary reflector at three different positions (BUS 36+000-PANEL, BUS 16+000 PANEL and BUS 36+000-BEAM, for more details see the PTCS wiki); rms of the temperature registered by different sensors located over the GBT; wind speed recorded by two weather stations, weather 2 is located in the ground, weather 3 is located on the feed arm of the GBT; acceleration recorded by accelerometer 1 (located on top of the receiver cabin) in the z direction (vertical displacement); displacements of the feed arm in the elevation and its orthogonal direction recorded by the quadrant detector (QD). The orange dotted line marks sunset (8:43 PM EDT, Sun's elevation $-50'$), while the purple dotted line marks sunrise (5:55 AM EDT, Sun's elevation $-50'$).

4.2 24 hour scan

The goals of the 24 hour scan were to determine; (i) what noise levels is it possible to reach using the TLS, (ii) what external factors (e.g., wind, differential heating) affect the accuracy of the TLS measurements, and (iii) how long does the surface error of the primary remain below 230 μm.

An animation showing the results of the 24 hour scan can be found here. This animation shows the scan-to-scan variations on the GBT's primary as seen by the TLS. A panel in the bottom shows the value of the scan-to-scan rms as a function of time.

To answer question (i) we measured the scan-to-scan rms of the primary between pairs of consecutive scans. For each pair of scans the first scan acts as reference while the later scan is the signal. The reference is subtracted from the signal scan and the rms is computed over the primary's surface. These measurements are presented in the top panel of Figure 2. There we can see that between sunset (20:45 hrs EDT) and 9 AM of the next day the scan-to-scan rms remains close to 200 μm, reaching a minimum value of 188 μm at 4:30 AM. A scan-to-scan rms of 200 μm corresponds to a LASSI noise of ≈ 150 μm.

To answer question (ii) we compared the scan-to-scan rms, used to answer the previous question, with external factors recorded by the sensors installed on the GBT (the weather 2 station is not on the telescope itself). This comparison is presented in Figure 2. There we can see that between sunset (20:45 hrs EDT) and 9 AM of the next day the scan-to-scan rms remains close to 200 μm. During this same period the wind speed remains below 3 m s^{-1}. Then, after 10 AM, the measured scan-to-scan rms jumps from ≈ 200 μm to ≈ 700 μm right at the time the wind speed is higher than 6.6 m s^{-1}. By comparison, between sunrise and 10 AM, the temperature over the GBT's primary gradually rises from 5 °C to 21 °C, while the rms between pairs of scans remains almost constant. This suggests that vibrations on the feed arm induced by the wind are the main limiting factor when measuring the surface rms using the TLS. The effect of the wind on the ability to correct the GBT's primary surface is analyzed in §4.3.3.

To answer question (iii), we assume that the scan-to-scan rms is a factor of $\sqrt{2}$ larger than the surface error, i.e. the GBT's primary represents a perfect paraboloid during the reference scan. In this case a surface error of 230 μm corresponds to a scan-to-scan rms of 330 μm. We use three different scans as reference, one close to 13:00 hrs on June 11, one at 00:30 hours and another at 6:10 AM. The first two reference scans represent two opposite extremes in the measured scan-to-scan rms during the 24 hour scan, while the third scan represents a situation with low wind speeds during day time. The measured scan-to-scan rms using these three scans as references are presented in Figure 3.

When we use a reference scan with large noise (top panel of Figure 3), the large noise is transferred to the surface deformation map, resulting in larger values of the scan-to-scan rms. When we use a reference scan with low noise (middle panel of Figure 3), we can see how the scan-to-scan rms slowly changes over time. This slow change at first shows how the primary changes as the structure slowly cools down, while the more rapid increase in the rms after sunrise reflects the influence of heating. After around 9 AM, the wind speed increases producing a larger scatter in the measured surface rms. During night time the scan-to-scan rms remains below 330 μm until 30 minutes after sunrise. The bottom panel of Figure 3 shows that during day time the scan-to-scan rms increases to > 330 μm after one hour and 30 minutes.

During the day time portions of the 24 hour scan the skies were clear. At around 7 AM half of the GBT's primary is directly illuminated by the Sun. At that time we observe no significant increase in the scan-to-scan rms. This suggests that the increased uncertainty in the TLS measurements due to direct illumination of the surface by the Sun is not significant.

4.3 Correcting deformations

4.3.1 Deformation applied to the active surface

For both the reference and signal scans a parabola was fitted. The residuals between these parabola fits and the scans are then subtracted to create a surface deformation map, shown in Figure 4. The surface deformation map should only contain the Zernike polynomial reproduced by the active surface and noise a factor of $\sqrt{2}$ larger than the surface error of the primary (≈ 230 μm, Frayer et al., 2018) plus TLS noise.

In this deformation map we determine the coefficients of the Zernike polynomials present. The coefficients of the first 36 Zernike polynomials recovered from the deformation map are shown in Figure 5. There we can see that the Zernike 6 (Z6) term has the largest coefficient, 0.89 mm, followed by Z3 (vertical tilt) with -0.68 mm. The remaining polynomials show coefficients which are consistent with noise (amplitudes < 580 μm).

After subtracting the fitted Zernike polynomials from the deformation map (middle and left panels in Figure 4, respectively) the rms is 307 μm. This corresponds to a LASSI noise of 217 μm, a 45% larger than the LASSI noise during night time (§4.2). We attribute this difference to the presence of radial stripes in the residuals (right panel in

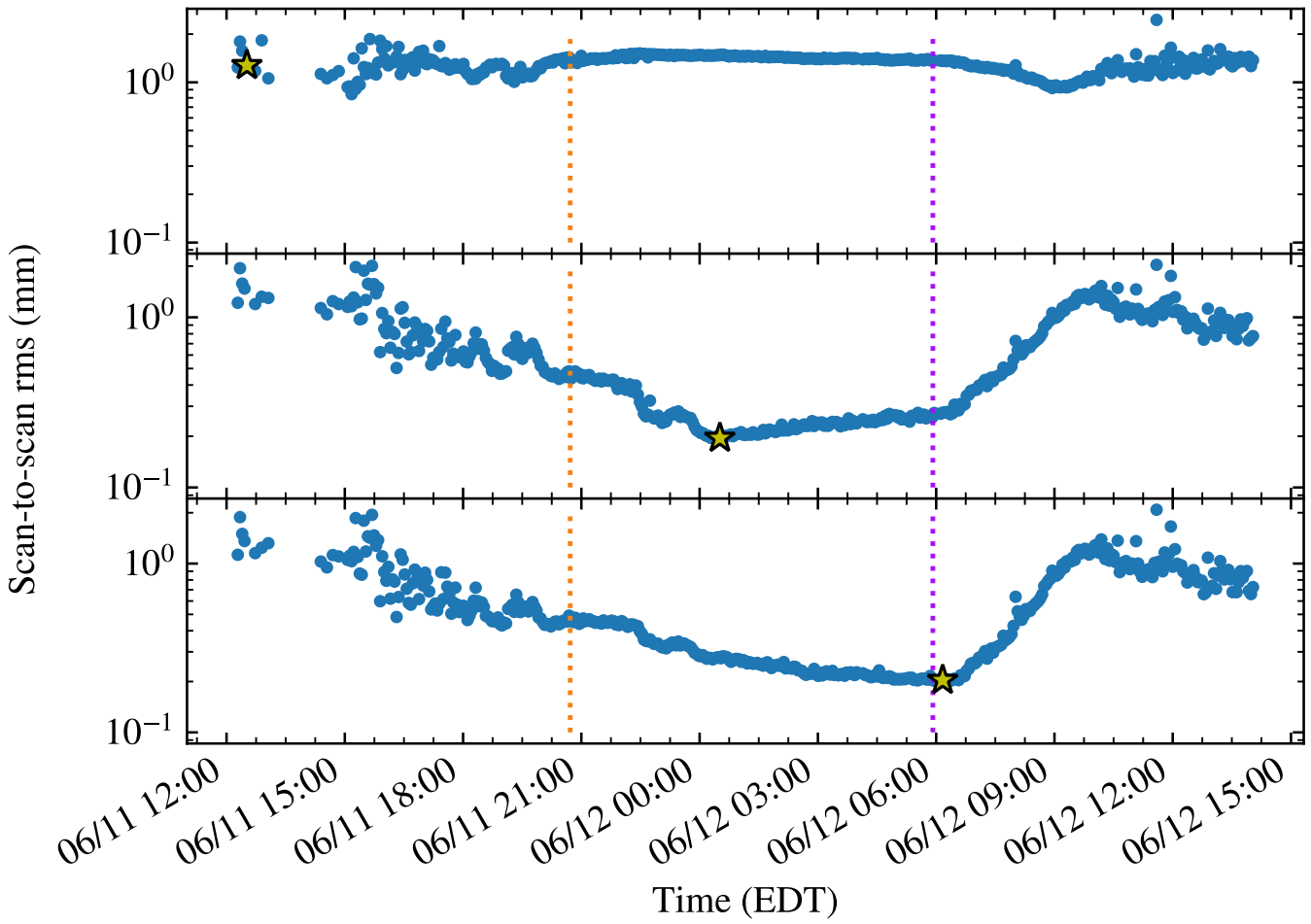

Figure 3: Measured scan-to-scan rms as a function of time using three different scans as reference scans. The top panel shows the scan-to-scan rms when a scan taken close to 13:00 hrs on June 11 is used as reference (high rms case). In the middle panel a scan taken at 00:30 hours is used as reference (low rms case). The orange dotted line marks sunset, while the purple dotted line marks sunrise. In the bottom panel the reference scan is taken at 6:10 AM. After one hour and 30 minutes the scan-to-scan rms is above 330 μm. The yellow stars mark the time at which the reference scan was taken.

Figure 4). These radial stripes are produced by the movement of the TLS with respect to the GBT's primary, likely caused by the vibration of the GBT's feed arm due to the wind.

4.3.2 Thermal deformations during the 24 hour scan

During the 24 hour scan the primary's surface will continuously change due to thermal gradients. We used this to simulate how the TLS generated scans will be used to correct the primary's surface. We used the last two reference scans in Figure 3 (middle and bottom panels) as examples of night and day time conditions. Then, we compared subsequent scans (signal scans) to these reference scans. By taking the difference between a signal and reference scan we generate deformation maps. From the deformation map we recover the deformations, expressed as the coefficients of Zernike polynomials. The recovered deformations are then subtracted from the deformation map to produce a corrected surface where we measure the rms. A diagram showing the workflow is presented in Figure 6.

Night time referenced scans

To test how long a night time reference scan remains valid we used the scan taken at 00:30 AM as reference (middle panel of Figure 3) and scans taken at different times as signal. For each signal scan we measured the rms after subtracting the Zernike polynomials recovered from the deformation maps. A summary of this is presented in Figure 7.

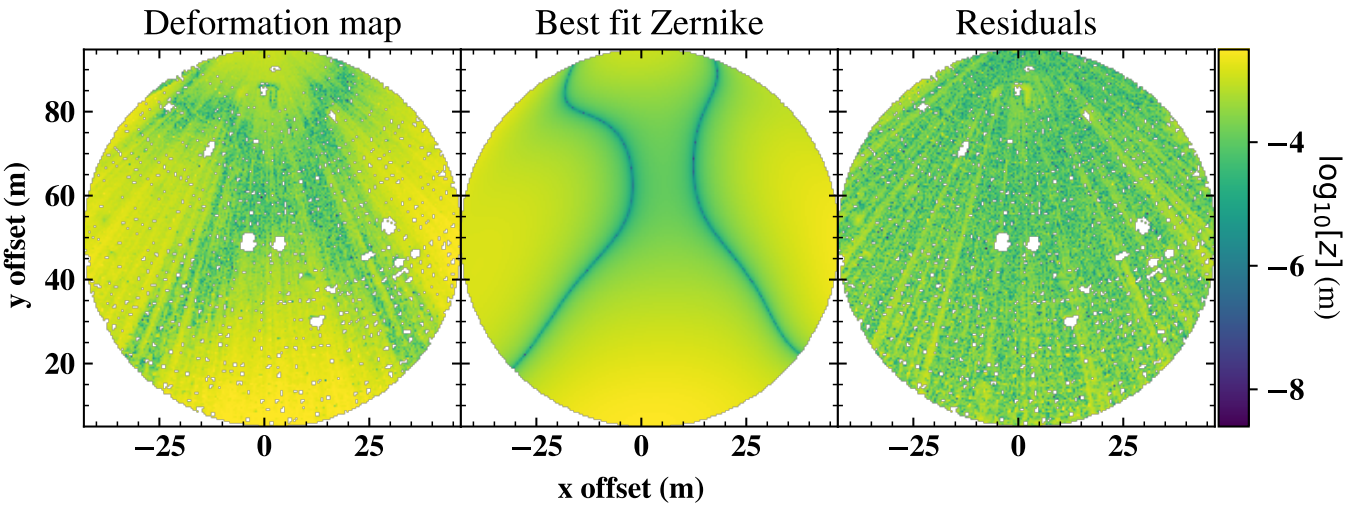

Figure 4: Results from the experiment performed during March 27, 2019. The active surface on the GBT's primary was commanded to reproduce a Zernike polynomial of index 6 with an amplitude of 1.7 mm. The masked regions within the primary reflector correspond to retroreflectors and displaced panels present during the experiment. The rms of the residuals is 307 μm.

Day time referenced scans

To test how the situation changes during day time we used a scan taken at at 6:10 AM (same as in the bottom panel of Figure 3) as reference. Figure 7 shows that the rms of the residuals increases faster than during night time. After 140 minutes, the rms of the residuals is larger than 230 μm, which implies that a reference scan taken during the morning can remain valid for up to two hours. The rms of the residuals is a factor of 2–3 lower than that in the deformation maps.

4.3.3 Simulated deformations

24 hour scan

To further test the capabilities of the TLS generated maps for recovering deformations in the GBT's primary we also injected simulated deformations into the 24 hour scans. As deformation, we used the linear superposition of the Zernike polynomials of index 4 to 21 with the coefficients of Figure 1. This deformation introduces a surface error of 198 μm, and is representative of a typical deformation encountered in the GBT's primary. The injected deformation is added to the unknown thermal deformations present in the primary during the 24 hour scan. This is the same procedure as used in §4.3.2, but adding a known deformation to the signal scans. The results from this analysis are presented in Figure 7 as green and blue crosses for day and night time referenced scans, respectively.

For two of the signal scans, four and eight hours after the night time reference scan, we also show the coefficients of the Zernike polynomials recovered from the deformation maps, Figure 8. For the scan taken four hours after the reference (4:30 AM), the recovered coefficients of the Zernike polynomials closely match the input as there is almost no thermal distortion of the primary during this time. For the scan taken eight hours after the reference (8:30 AM), the coefficients are different by 3000% and 50% for Z6 and Z4, respectively. This reflects the effect of the thermal deformation of the GBT's primary during day time. Higher order terms, Zernike polynomials of indices larger than 10, represent smaller scale deformations on the primary, hence they are not well correlated with thermal deformations. In particular we see that for Z14, Z18 and Z21 (the higher order terms with the largest coefficients) the difference between the recovered and input coefficients is smaller than 50% for the scans four hours apart. Their coefficients are 40 μm, -57 μm and -55 μm.

Wind effect

To determine how does the wind, and the shaking of the feed arm, affect our ability to correct the GBT's primary surface we injected simulated deformations into the 24 hour scan (Figure 6). We used subsequent pairs of scans as reference and signal. As deformation we used a Z6 with a coefficient of 300 μm.

The LASSI noise as a function of wind speed and displacement of the feed arm is presented in Figure 9. This Figure shows that for wind speeds lower than 2.7 m s^{-1} (6 mph), the LASSI noise is $\lesssim 300$ μm. Here we use the rms

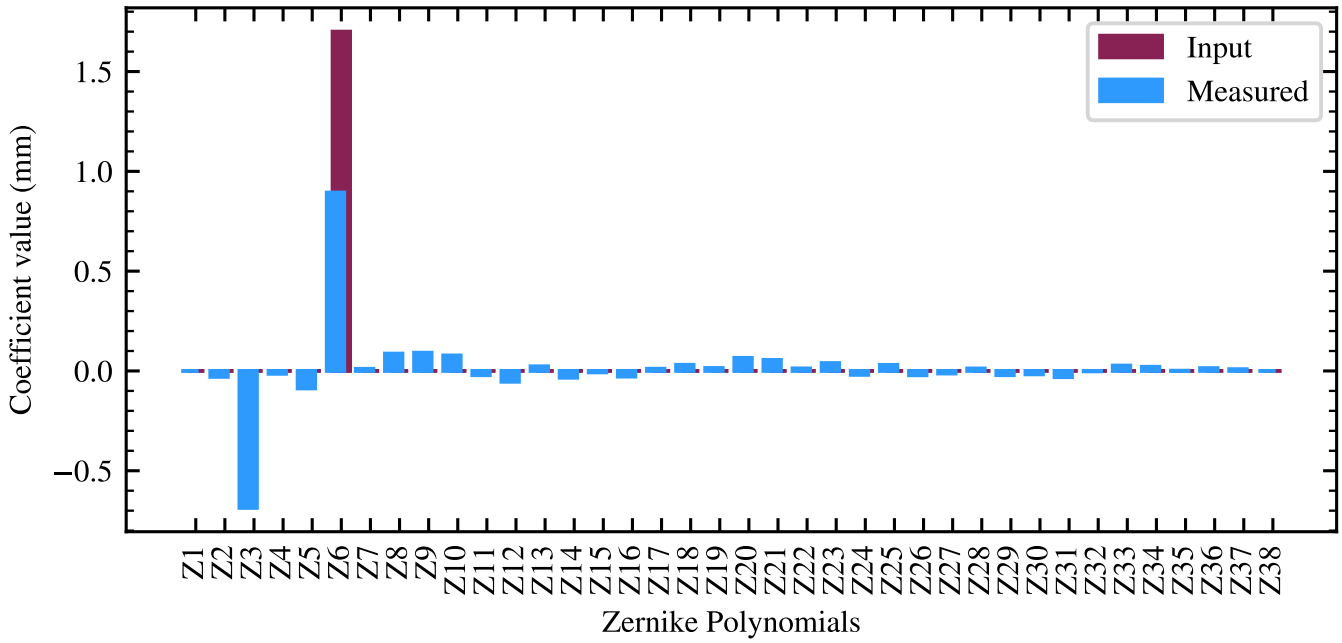

Figure 5: Coefficients of the Zernike polynomials recovered from the deformation map for the experiment performed during March 27 (Figure 4).

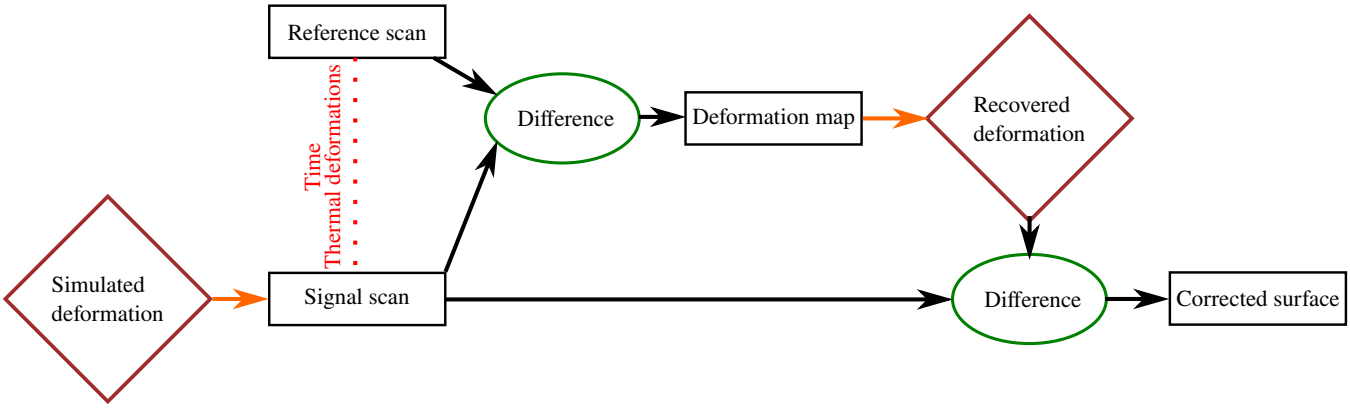

Figure 6: Diagram showing how a signal and reference scan are used to simulate correcting the GBT's primary surface.

in the residuals of the surface deformation maps with respect to the recovered Zernike polynomials as a proxy for the LASSI noise.

Amplitude threshold for significant Zernike coefficients

We used two scans taken at 2 AM to test what is the minimum coefficient we can recover using the TLS generated surface maps. In the signal scan we injected a Zernike polynomial where only Z4 is not zero. The coefficient of Z6 was varied until its recovered value was smaller than three times the rms of the recovered coefficients. The lowest value of Z6 that we can recover above this threshold is 15 μm, Figure 10. After subtracting the recovered Zernike polynomials from the deformation map, the rms dropped from 236 μm to 233 μm.

5 Summary

The goal of the LASSI project is to increase the number of hours available for high frequency observations ($>$ 25 GHz) with the GBT through the use of a TLS. The scans from the TLS will be compared to a reference surface to measure thermal deformations in the GBT's primary. Based on the proposed solution, obtaining the reference surface through

AutoOOF is the most time consuming overhead (25 minutes).

Here we have presented experiments performed using the TLS mounted on the roof of the receiver cabin of the GBT, similar to the proposed setup for science observations. These experiments show that the LASSI noise is ≈ 150 μm, under weather conditions favorable for high frequency observations (wind speeds lower than 2 m s^{-1}, Figures 2 and 9). With the TLS it is possible to detect Zernike polynomials with amplitudes of ≈ 15 μm (Figure 10) in the surface of the GBT.

To determine how long a reference surface remains valid we simulated thermal deformations in the GBT's primary. These thermal deformations were added to maps of the GBT's primary which already contain the effect of thermal deformations. We then recovered the deformation from the difference between a reference scan and the scan were the deformation was simulated. The recovered deformations were used to correct the primary's surface. We find that during night time the reference scan remains valid ≈ 7.5 hours, i.e., we can correct the surface with a LASSI noise < 230 μm. During day time the reference scan remains valid for two hours.

The current analysis is limited by the presence of wind speeds larger than 6.6 m s^{-1} during the day time. Future day time tests should allow us to better understand what is the time cadence necessary to keep the surface error below 230 μm. The current data suggests that the surface error remains below 230 μm for periods of less than an hour and a half if thermal distortions are not compensated during the morning.

"Enhancing GBT Metrology to support high resolution 3mm molecular imaging for the U.S. Community" is supported by the National Science Foundation under Award Number AST-1836009.

References

Born, M., L. Born, E. Wolf, M. BORN, A. Bhatia, P. Clemmow, D. Gabor, A. Stokes, A. Taylor, P. Wayman, et al.
1999. *Principles of Optics: Electromagnetic Theory of Propagation, Interference and Diffraction of Light*. Cambridge University Press.

Frayer, D. T., F. Ghigo, and R. J. Maddalena
2018. GBT memo #301: The GBT Gain Curve at High Frequency.

Holst, C., T. Artz, and H. Kuhlmann
2014. Biased and Unbiased Estimates Based on Laser Scans of Surfaces with Unknown Deformations. *Journal of Applied Geodesy*, 8:169–184.

Holst, C., A. Nothnagel, M. Blome, P. Becker, M. Eichborn, and H. Kuhlmann
2015. Improved area-based deformation analysis of a radio telescope's main reflector based on terrestrial laser scanning. *Journal of Applied Geodesy*, 9:1–14.

Holst, C., P. Zeimetz, A. Nothnagel, W. Schauerte, and H. Kuhlmann
2012. Estimation of focal length variations of a 100-m radio telescope's main reflector by laser scanner measurements. *Journal of Surveying Engineering*, 138(3):126–135.

Hunter, T. R., F. R. Schwab, S. D. White, J. M. Ford, F. D. Ghigo, R. J. Maddalena, B. S. Mason, J. D. Nelson, R. M. Prestage, J. Ray, P. Ries, R. Simon, S. Srikanth, and P. Whiteis
2011. Holographic Measurement and Improvement of the Green Bank Telescope Surface. *Publications of the Astronomical Society of the Pacific*, 123:1087–1099.

Nikolic, B., R. M. Prestage, D. S. Balser, C. J. Chand ler, and R. E. Hills
2007. Out-of-focus holography at the Green Bank Telescope. *Astronomy and Astrophysics*, 465(2):685–693.

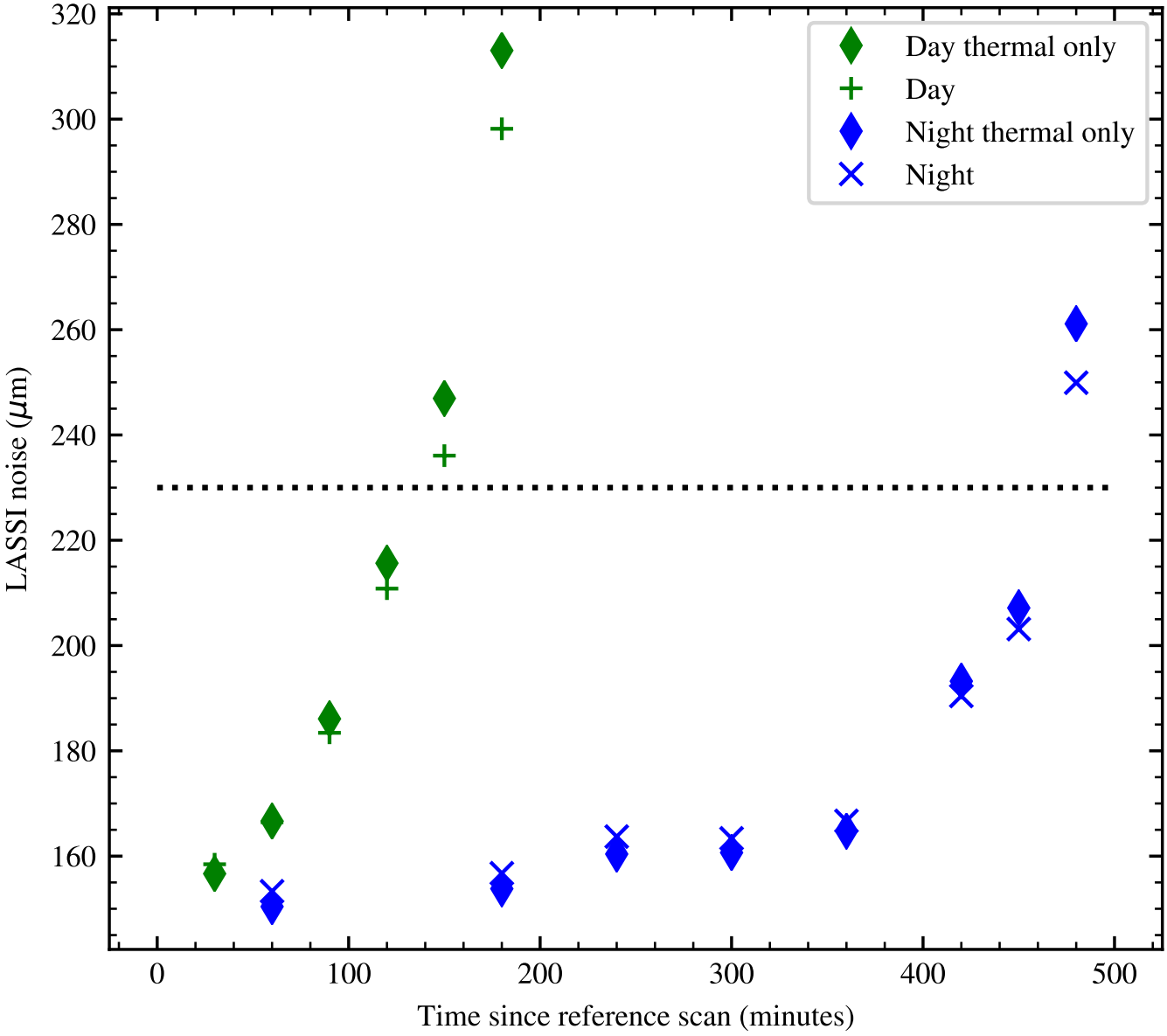

Figure 7: LASSI noise after subtracting the Zernike polynomials recovered from the deformation maps. The green symbols show the results when the reference scan was taken at 6:10 AM. The green crosses correspond to values obtained when we incorporate simulated deformations into the scans, while for the green diamonds no simulated deformations were added. The blue symbols show the results when the reference scan was taken at 00:30 AM. The blue crosses correspond to values obtained when we incorporate simulated deformations into the scans, while for the blue diamonds no simulated deformations were added. Here we have taken out the factor of $\sqrt{2}$ present in the residuals.

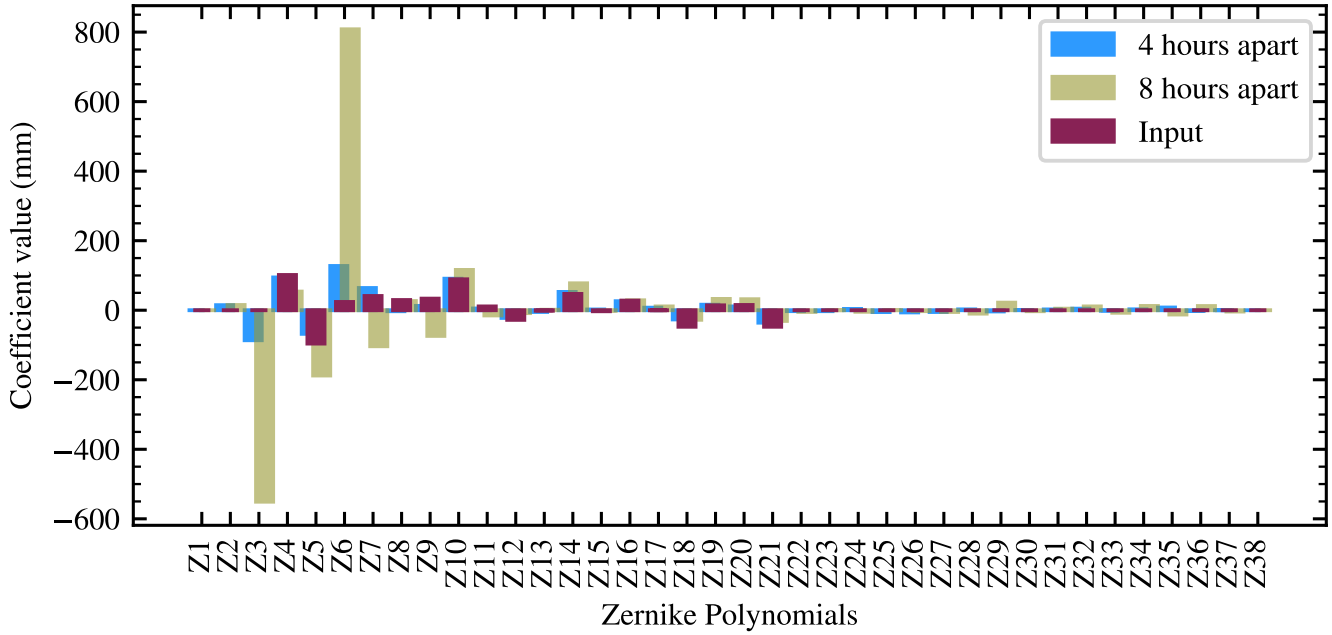

Figure 8: Comparison between the coefficients of the Zernike polynomials used to generate a signal scan, and the coefficients recovered from the surface deformation map when the signal and reference scan are separated by four and eight hours. In both cases the rms dropped after subtracting the Zernike polynomial generated from the recovered coefficients. For the scans four hours apart the rms dropped from 346 μm to 231 μm, while for those eight hours apart it dropped from 1100 mm to 0.35 mm.

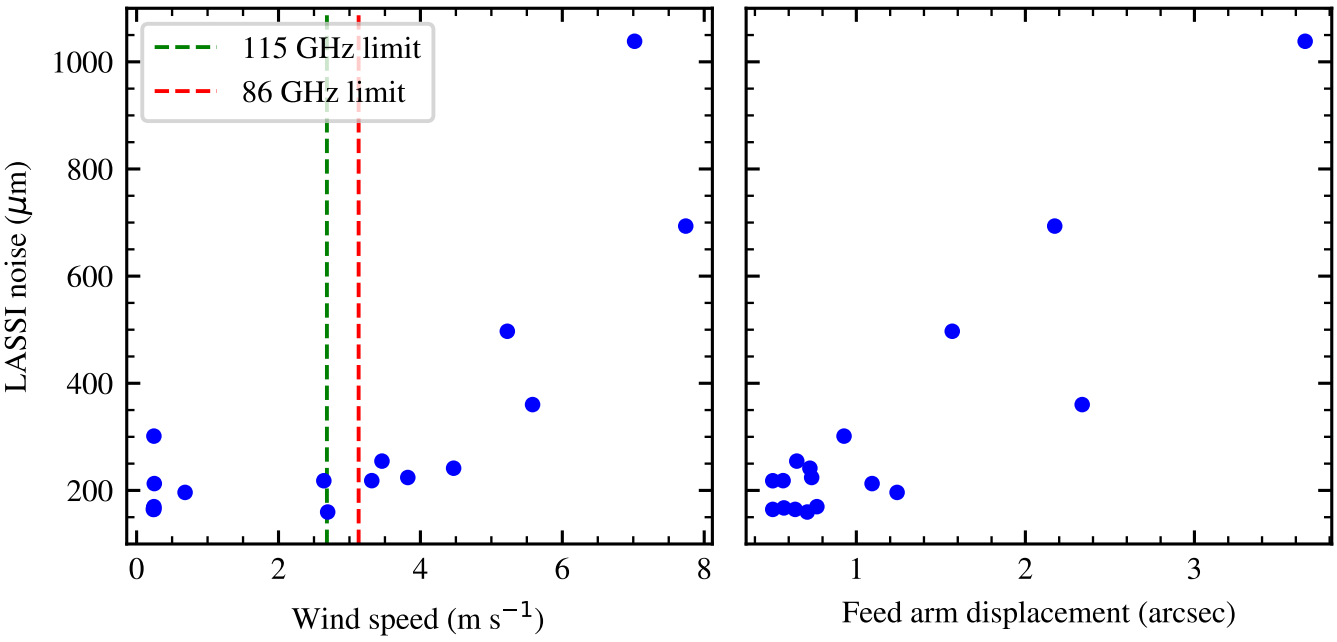

Figure 9: LASSI noise as a function of wind speed (left panel) and displacement of the feed arm (right). The green and red dashed vertical lines show the wind speed limits for observations at 115 GHz and 80 GHz, respectively. These limits are taken from Figure 17.1 in the GBT observers guide, used by the dynamic scheduling system.

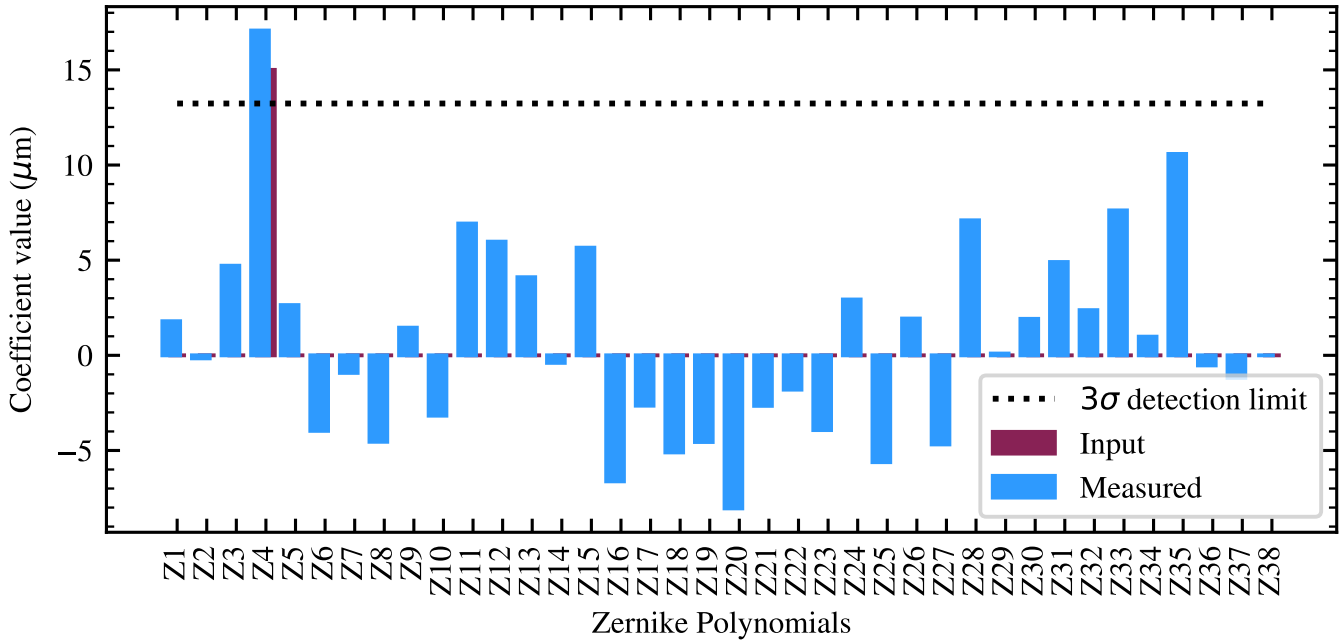

Figure 10: Lowest coefficient for Z4 that we can recover. The difference between the simulated coefficient and the recovered value is 13 %.

A AutoOOF derived Zernike coefficients

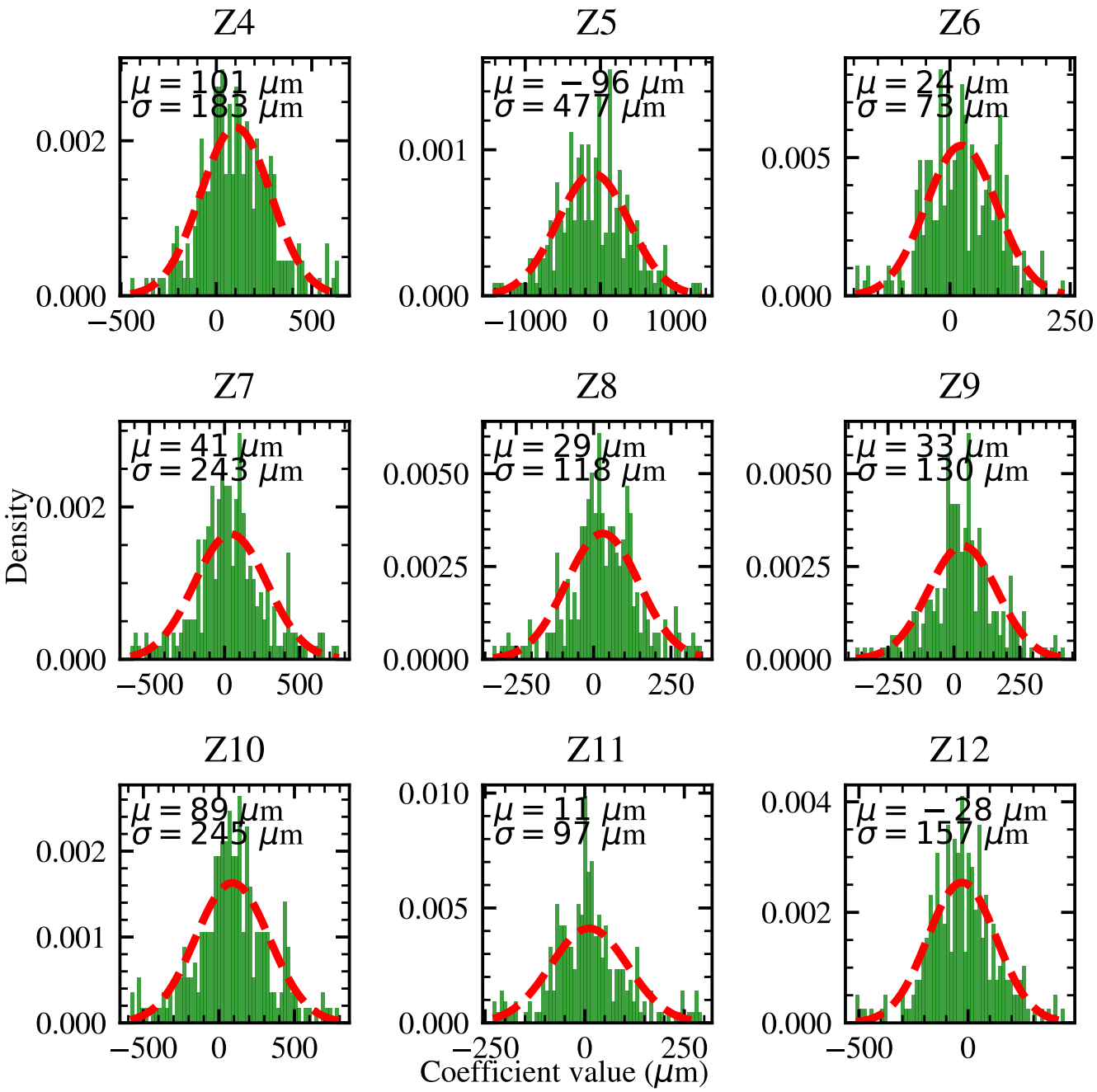

Figure 11: Histogram showing the values of the coefficients for the Zernike polynomials derived using *AutoOOF*.

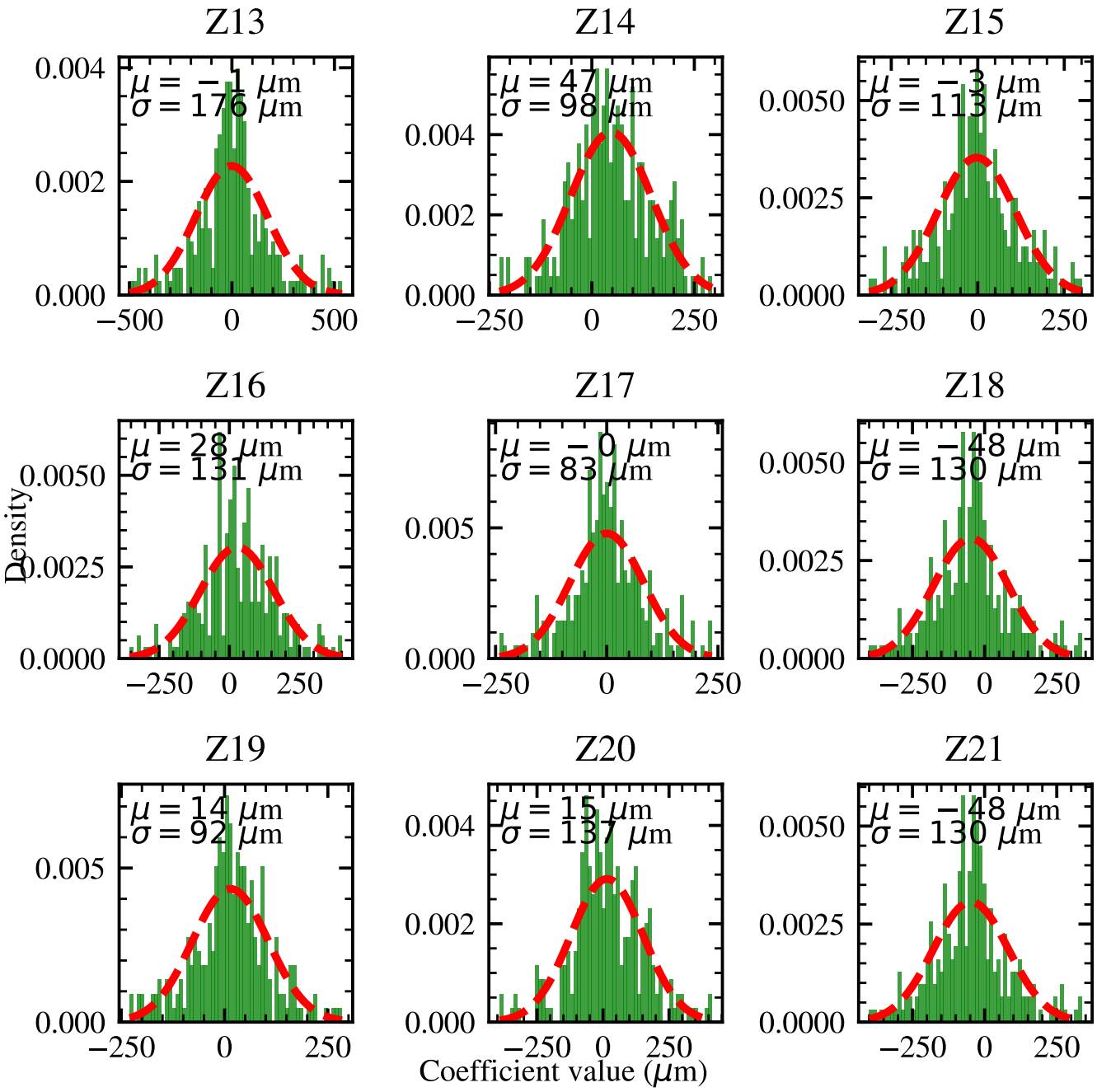

Figure 12: Figure 11 continued.